Proceedings of the ASME 2022 International Technical Conference and Exhibition on Packaging and Integration of Electronic and Photonic Microsystems
InterPACK2023
October 24-26, 2023, San Diego, California

IPACK2023-111917

DEVELOPMENT OF CERAMIC PULSATING HEAT PIPES FOR MEDIUM-VOLTAGE POWER ELECTRONICS

Ramy Abdelmaksoud, Jeffrey Diebold, Sai Kiran Hota, and Kuan-Lin Lee
Advanced Cooling Technologies, Inc.
Lancaster, PA

Shivangi Sinha and Dragan Maksimovic
University of Colorado, Boulder
Boulder, CO

ABSTRACT

Due to the rapid increase of electric vehicles in the market, a corresponding significant increase in fast chargers will be needed. However, expanding the adoption of fast chargers such as direct current fast chargers is challenging with the current grid infrastructure. Medium-voltage (MV) electronics are an essential component in grid-tied applications. However, thermal management of such components presents a barrier to pushing the boundaries of high-power density, while maintaining high efficiency and reliability. Thermal management is further complicated by the need to maintain sufficient voltage isolation. Under a Small Business Innovative Research (SBIR) Phase I program funded by the U.S. Department of Energy (DOE), Advanced Cooling Technologies, Inc. (ACT), in collaboration with the University of Colorado, Boulder (UC Boulder) developed innovative ceramic Pulsating Heat Pipes (PHP)s, which significantly improved the thermal management and provided voltage isolation. Different flat ceramic PHPs were fabricated for the lab-scale testing. The thermal performance and voltage isolation were evaluated through both experimental testing and numerical modeling. The effect of different parameters, such as the fill ratio, gravity-aided and against-gravity orientations, and heat input, on the thermal performance of the ceramic PHP, was investigated. It was found that at the optimal fill ratio, a thermal resistance reduction of 41%-67% was achieved for different gravity-aided orientations (0-90˚) when compared to the uncharged ceramic PHP (i.e., the ceramic PHP without fluid in it). The ceramic PHP was able to efficiently transport up to 6 W/in^2 with a thermal resistance reduction of 58% at the horizontal position. The voltage isolation testing showed that the ceramic PHP can provide electrical insulation when exposed to a voltage of 28 kV. In addition, the effect of different working fluids and fill ratios, on the voltage isolation capability of the ceramic PHP, was investigated.

Keywords: Thermal Management, Ceramic, Pulsating Heat Pipes, Voltage Isolation

NOMENCLATURE

D_{cr}	Critical channel diameter
g	Gravitational constant
Q	Heat transport
T_{sat}	Saturation temperature of working fluid
ΔT	Temperature difference between the evaporator and condenser
μ_l	Viscosity of liquid
ρ_l	Liquid density
ρ_v	Vapor density
σ	Surface tension

1. INTRODUCTION

1.1. Medium-Voltage Power Electronics

Due to the current efforts of electrification (i.e., replacing technologies that use fossil fuels with technologies that use electricity as a source of energy), significant modifications to the current grid infrastructure are needed. Electrification is being implemented in different applications such as transportation, residential, commercial, etc. Transportation electrification can be considered the most challenging since the wide EV adoption is restricted by the availability of fast charging systems. For example, there is currently a focus on developing the power electronics necessary to enable cost competitive Direct Current Fast Charging (DCFC) (480V, 50–150kW) and even more ambitious Extreme Fast Charging (800+V, 400kW) [1]. In order

to fulfill those electrification efforts, high-power density medium-voltage power electronics are needed. However, as with many power electronics, thermal management presents a barrier to enabling high-power density electronics, while maintaining high efficiency and reliability. Thermal management for MV devices is further complicated by the need of having the thermal management system in direct contact with the MV regions for low thermal resistance and consequently still maintain sufficient voltage isolation.

1.2. Pulsating Heat Pipes (PHPs)

A Pulsating Heat Pipe (PHP), also called Oscillating Heat Pipe (OHP), is a passive two-phase heat transfer device that was first introduced in 1990 by Akachi [2]. A PHP is typically made up of a plain long meandering tube (or channel) of capillary dimensions with many U-turns joined end-to-end. The serpentine is partially charged with a working fluid and hermetically sealed. Due to capillary forces, working fluid naturally distributes in the form of liquid-vapor slugs as shown in FIGURE 1.

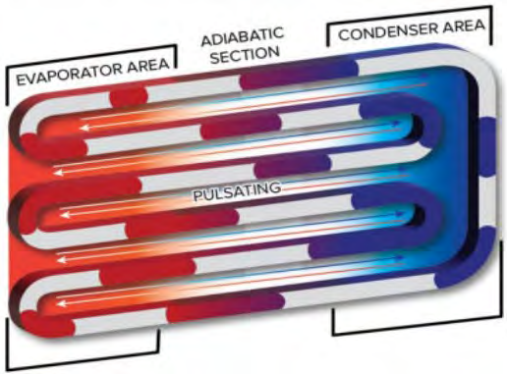

FIGURE 1: SCHEMATIC OF THE OPERATION MECHANISM OF A PULSATING HEAT PIPE (PHP)

Heat transfer from the heated end (i.e., evaporator) to the cooled end (i.e., condenser) is achieved by the oscillating action of slugs and plugs. The basic operation principle of a PHP is described as follows:

- Heat entering the evaporator vaporizes the working fluid inside. This causes an increase in vapor pressure and the expansion of vapor bubbles in the evaporation section.
- Simultaneously, vapor bubbles in the cooling section condense and shrink, which leads to the decrease of vapor pressure at the condenser.
- The growth and shrinkage of bubbles in the heated and cooled sections will push the liquid slugs in between from the evaporator to the condenser. This is considered to be the major driving force of the PHP.
- Because of the interconnection of the tubes, the motion of the liquid slugs and vapor bubbles at one section of the tube towards the condenser also leads to the motion of slugs and bubbles in the other section (i.e., towards the evaporator). This works as the resorting force of the PHP.
- The inter-play between the driving force and restoring force leads to the oscillating action of the vapor bubbles and the liquid slugs.
- Heat is carried by the oscillating motion of the fluid from the evaporator to the condenser.

PHPs are passive heat transfer devices with effective thermal conductivities as high as 1000 – 2000 W/m·K [3], 5-10x higher than aluminum and 2-5x higher than copper. They can be designed with complex external geometry including out-of-plane bends, complex internal geometry guiding heat to specific locations and are amenable to 3D printing. PHPs can be fabricated from a variety of materials such stainless steel and aluminum. Compared to other, more conventional passive two-phase heat transfer devices, such as heat pipes and vapor chambers, the PHP has several advantages for the current application.

- PHPs do not require a wick structure to provide capillary pumping of the liquid.
- PHPs take advantage of both sensible and latent heat transfer of working fluid, which will provide order-of-magnitude thermal conductivity enhancement compared to aluminum and copper.
- PHP channels can accommodate complex geometry.
- PHPs can be much thinner than traditional heat pipes.
- PHPs can operate effectively in any orientation.

PHP working fluid selection depends predominantly on the operating temperature, PHP size and the desired thermal performance. The PHP size parameters include the channel diameter, number of turns, and overall dimensions. The channel diameter should be always less than the critical diameter which is the maximum diameter that can allow the vapor plugs and liquid slugs to oscillate (maintain a pseudo balance between the surface tension and gravity force). If the channel diameter is larger than the critical diameter, the gravity force will dominate (i.e., liquid slugs will not be able to keep attached to the surface), while if the diameter is too small, the surface tension dominates (i.e., the hydraulic resistance increases significantly, and the slugs will not be able to oscillate). The critical diameter can be defined by the following formula where σ is the surface tension (N/m), g is the acceleration due to gravity, ρ_l is the liquid density, and ρ_v is the vapor density.

$$D_{cr} = 2\sqrt{\frac{\sigma}{g(\rho_l - \rho_v)}} \quad (1)$$

Several working fluid transport factors, which are thermo-physical property relations in the corresponding heat transfer limits were used to simplify the working fluid selection. These property relations are described in detail by Drolen and Smoot [4]. PHP start-up is another important parameter affecting the performance of PHP. A start-up transport factor, based on the minimum start-up heat flux equation provided by Taft et al., [5] was used.

ACT has several ongoing programs developing PHPs for various applications. In an ongoing SBIR Phase II program

funded by NASA, ACT is developing a PHP heat spreader for standard 3U form factor electronics (space modular electronics) thermal management [6, 7]. An extensive comparison between PHP and other high thermal conductivity heat spreaders (e.g., HiK™ plates) can be found in [8-10].

The objective of this paper is to report the research effort that investigated the feasibility of using a passive two-phase heat transfer device (ceramic PHP) for removing the waste heat from MV electronics efficiently while providing voltage isolation.

2. Materials and Methods

2.1. The Ceramic PHP Design

2.1.1. Envelope Material

As mentioned before, it is challenging to have a device with high effective thermal conductivity that simultaneously provides voltage isolation since the vast majority of the materials that have good thermal conductivity have good electrical conductivity as well. Certain ceramic materials, such as alumina (aluminum oxide), have acceptable thermal conductivity and low electrical conductivity (i.e., serve as electrical insulator) which makes them an ideal candidate for such applications. The envelope material of the proof-of-concept design was selected to be made of alumina due to the following properties:

- Thermal conductivity (29-39 W/m·K)
- Breakdown strength (10-100 kV/mm)
- Suitable for different machining processes (e.g., 3D printing and milling)

2.1.2. PHP Parameters and Working Fluid Selection

The first step was to identify potential working fluids. Since the application requires dielectric fluids, refrigerants were considered due to their good thermal performance and dielectric properties. FIGURE 2 shows the critical diameter values at different operating temperatures for different working fluids. The critical diameter is the maximum diameter that can allow the vapor plugs and liquid slugs to oscillate. If the channel diameter is larger than the critical diameter, liquid slugs will not be able to stay attached to the surface, while if the diameter is too small, the hydraulic resistance increases significantly, and the slugs will not be able to oscillate. Typically, the efficiency and functionality of different electronics experiences significant negative effects if the operating temperature is ≥ 100˚C approximately. R-1233zd is a relatively new refrigerant and is being considered as a strong replacement to other refrigerants such as R-123 and R-134a due to its very low Global Warming Potential (GWP). R-1233zd has a GWP of 1 while R-123 and R-134a have GWP of 79 and 1430, respectively (as a reference, water has a GWP of 0). One more advantage of R-1233zd over common refrigerants such as R-134a is that it has much lower saturation pressure values which will reduce structural requirements of the ceramic and allow for thinner PHP envelopes (see FIGURE 3). A 2mm channel diameter was selected since it is below the maximum limit for a wide range of operating temperatures.

After the selection of the working fluid (i.e., R-1233zd), the heat transfer limits were calculated. FIGURE 4 shows the heat transfer limits of a 4″x4″ ceramic PHP when using R-1233zd as the working fluid. The fill ratio was assumed to be 25% and the heater and condenser areas are the same (i.e., 4″x1.25″). The area filled with dashed lines is the operating range of the ceramic PHP. The operating range should be higher than the start-up heat transfer limit and lower than all the other limits. Please note that the critical heat flux and viscous limits typically have very high values so that they are not included in FIGURE 4. Based on the calculated heat transfer limits, the 4″x4″ proof-of-concept ceramic PHP can easily transport over 50 W waste heat at various operating temperatures (e.g., at an operating temperature of 80˚C, the ceramic PHP will be able to remove up to 64 W). The thermal performance of the PHP can be improved (e.g., providing lower thermal resistance and higher maximum power) through different design modifications such as increasing the number of turns, maximizing the channel diameter (without exceeding the critical diameter), splitting the PHP into several smaller PHPs, choosing working fluids with high merit number, etc.

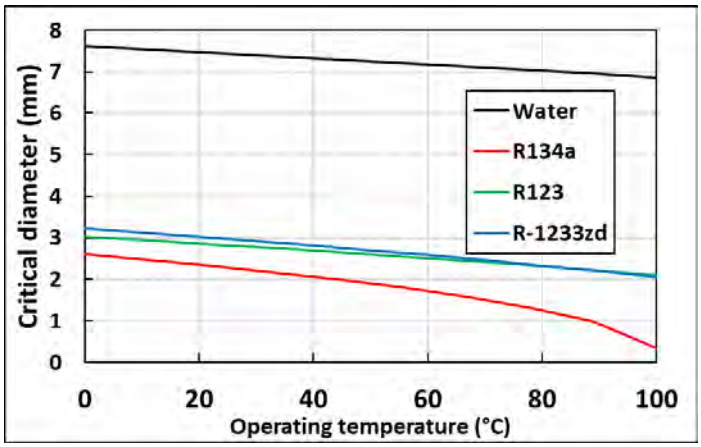

FIGURE 2: CRITICAL DIAMETER VALUES AT DIFFERENT OPERATING TEMPERATURES FOR DIFFERENT WORKING FLUIDS

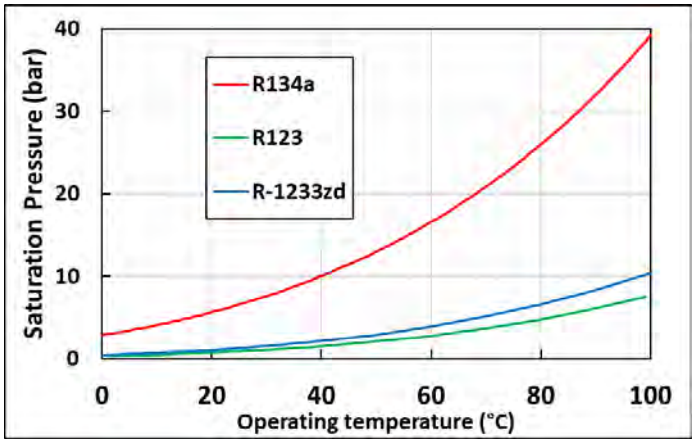

FIGURE 3: SATURATION PRESSURE AT DIFFERENT OPERATING TEMPERATURES FOR DIFFERENT WORKING FLUIDS

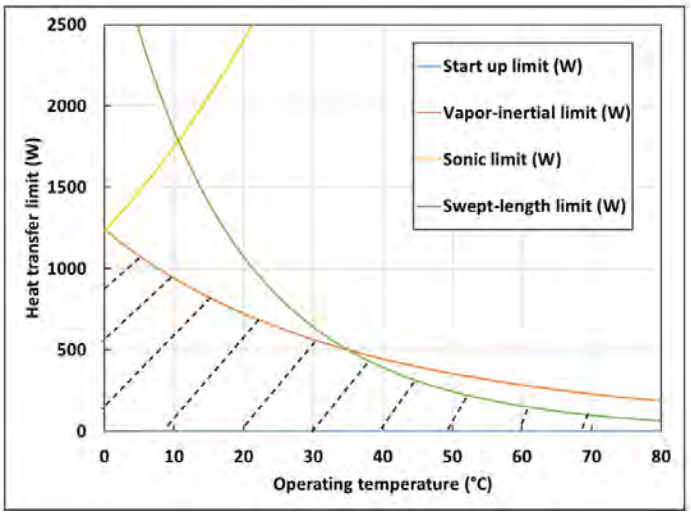

FIGURE 4: HEAT TRANSFER LIMITS FOR THE CERAMIC PHP WHEN USING R-1233ZD AS THE WORKING FLUID. THE AREA FILLED WITH DASHED LINES IS THE OPERATING RANGE OF THE CERAMIC PHP.

2.1.3. PHP Thermal Performance Prediction

To predict the thermal performance of the PHP, a theoretical heat transfer model was developed based on existing heat transfer correlations [4-5, 11-12]. The predicted PHP thermal resistance from the PHP model was used in a preliminary Finite Element Analysis (FEA) model in order to predict the temperature distribution along the ceramic PHP. FIGURE 5 shows a cut view of the CAD model of the proof-of-concept PHP design. The overall dimensions are 6" x 6" x 0.32". The PHP consists of 10 turns (i.e., 20 channels) where each channel has a diameter of 0.078" (i.e., 2mm). FIGURE 6 shows the temperature results of a preliminary FEA analysis of the ceramic PHP compared to a solid ceramic plate. A cold plate that consists of copper tubing and aluminum block is used as the heat sink (i.e., condenser). A heater block made from aluminum is used as the heat source (i.e., heater or evaporator). A heat rate of 50 W (to mimic the waste heat generated by the MV device) is applied on the heater. A convective heat transfer boundary condition is applied on the internal surface of the copper tubing (h=2,000 W/m^2·K with a temperature of 20˚C). Please note that the vapor/liquid space was modeled using a dummy material with high thermal conductivity based on the heat transfer model discussed above (i.e., 1,000 W/m·K). Using ceramic PHP provided a temperature reduction of 40˚C which translates into a thermal resistance reduction of 50%.

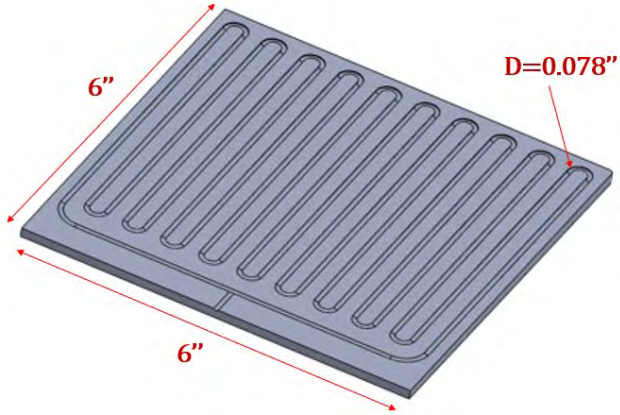

FIGURE 5: A CUT VIEW OF THE CAD MODEL OF THE PROOF-OF-CONCEPT PHP DESIGN. D IS THE CHANNEL DIAMETER.

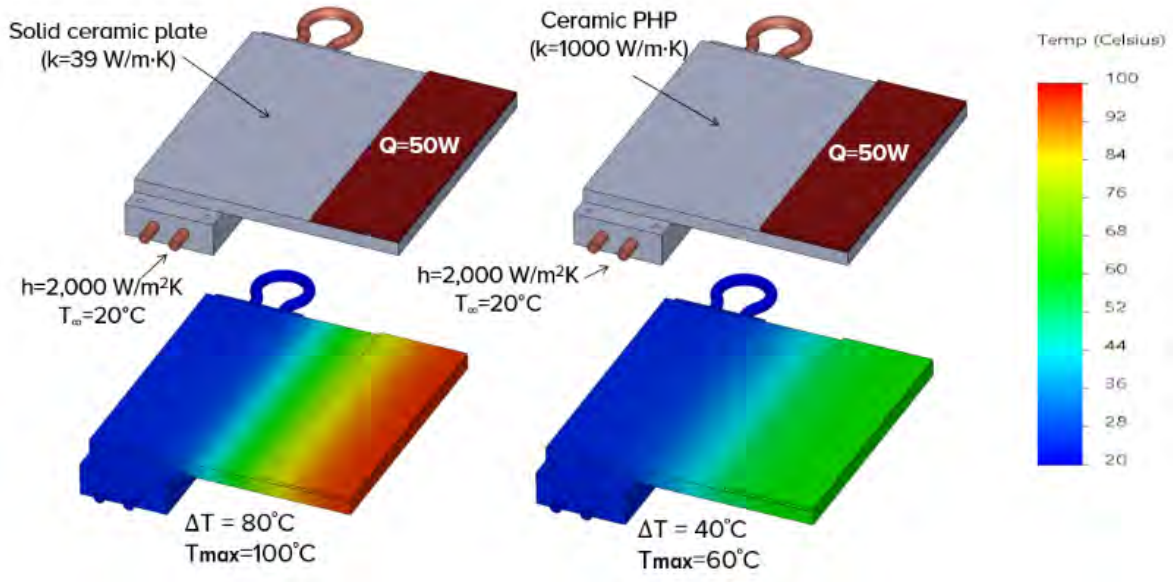

FIGURE 6: FEA ANALYSIS OF CERAMIC PHP AND SOLID CERAMIC PLATE

2.1.4. Fabrication of the Ceramic PHPs

Additive manufacturing (AM), or 3D printing, enables the fabrication of very complex geometries. However, ceramic 3D printing technology is not as mature as metal and plastic 3D printing technology. The most important characteristic of a two-phase flow device, such as the PHP, is to be hermetic in order to prevent any vapor or liquid leaks. Any vapor or liquid leaks would cause the two-phase flow device to stop functioning. ACT identified a ceramic 3D printing vendor capable of meeting these requirements. FIGURE 7 shows actual images and an X-ray of the 3D printed ceramic PHP. The X-ray was taken to make sure there is no blockage inside the 3D printed ceramic PHP channels.

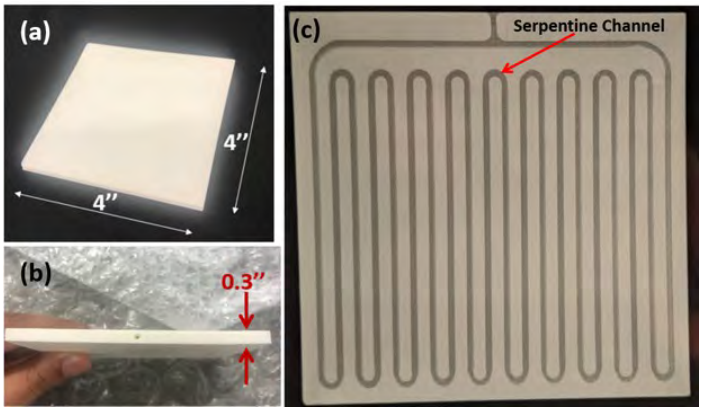

FIGURE 7: (A-B) IMAGES OF THE 3D PRINTED CERAMIC PHP. THE HOLE, IN (B), IS WHERE THE WORKING FLUID IS INJECTED. (C) AN X-RAY OF THE 3D PRINTED CERAMIC PHP.

In addition to the ceramic 3D printing approach, ACT also considered ceramic conventional machining (e.g., milling). The machined ceramic PHP was manufactured by bonding two ceramic plates where one is solid and the other has the PHP channels milled in it (see FIGURE 8). FIGURE 9 shows the actual images of the machined ceramic PHP.

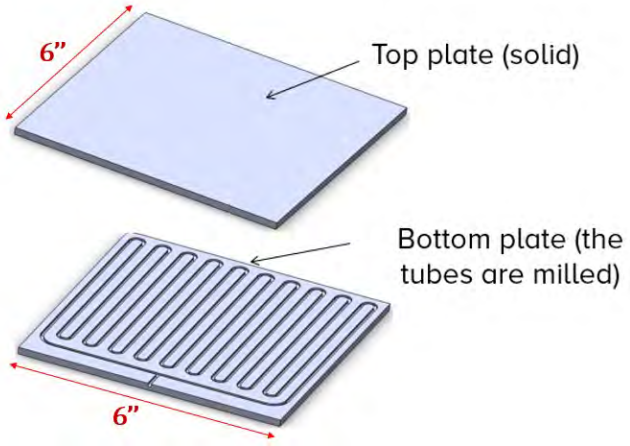

FIGURE 8: MACHINED CERAMIC PHP PLATES. THE HYDRAULIC DIAMETER OF THE CHANNELS IS 0.078’’ (2mm) AND THE TOTAL THICKNESS OF BOTH PLATES IS 0.32’’ (8mm).

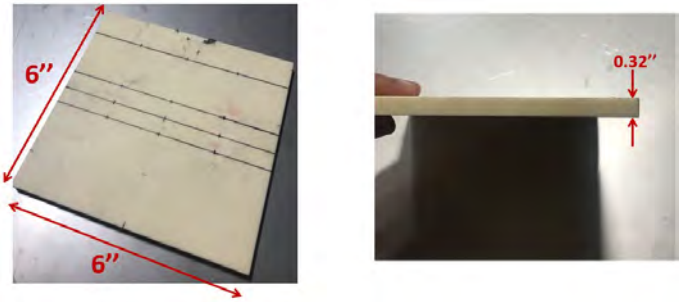

FIGURE 9: IMAGES OF THE MACHINED CERAMIC PHP. PLEASE NOTE THAT THE BLACK MARKING IS FOR THE THERMOCOUPLES INSTALLATION.

3. RESULTS AND DISCUSSIONS

3.1. Thermal Testing of the 3D Printed Ceramic PHP

3.1.1. Test Setup

FIGURE 10 shows the experimental setup before and after installing the insulation. The 3D printed ceramic PHP is mounted on a garolite plate (fiberglass insulation material). A cartridge heater (4” x 1.25”) and cold plate (chiller block) (4” x 1.25”) are clamped onto the PHP ends. The cartridge heater is connected to a power supply while the cold plate is connected to the chiller box. FIGURE 11 shows a top view of the thermocouples layout on the ceramic PHP.

3.1.2. Flow/Wall Conditions and Thermal Testing Process

A set of tests was performed for both the charged ceramic PHP and empty ceramic PHP (baseline). Charged ceramic PHP means that the ceramic PHP is partially filled with R-1233zd (working fluid) while empty ceramic PHP means that the PHP channels do not contain the working fluid. The testing process included the following tests:

- Horizontal position (under the design conditions: 21W)
- Horizontal position (higher power): 30 W “Q_{max}= 1.43 Q_{design}”
- Different orientations (15˚, 30˚, 90˚ “vertical”) (gravity-assisted heat source below heat sink)

TABLE 1 shows the experimental conditions of the charged and empty ceramic PHP. Please note that a fill ratio of 26% is 2 grams (0.004 lbs) of the working fluid (R-1233zd).

TABLE 1: EXPERIMENTAL CONDITIONS OF THE CHARGED AND EMPTY CERAMIC PHP

Parameter	Empty Ceramic PHP	Charged Ceramic PHP
Heat Input (W)	21	21
Sink Temperature (˚C)	5	5
Fill Ratio (%)	0	26

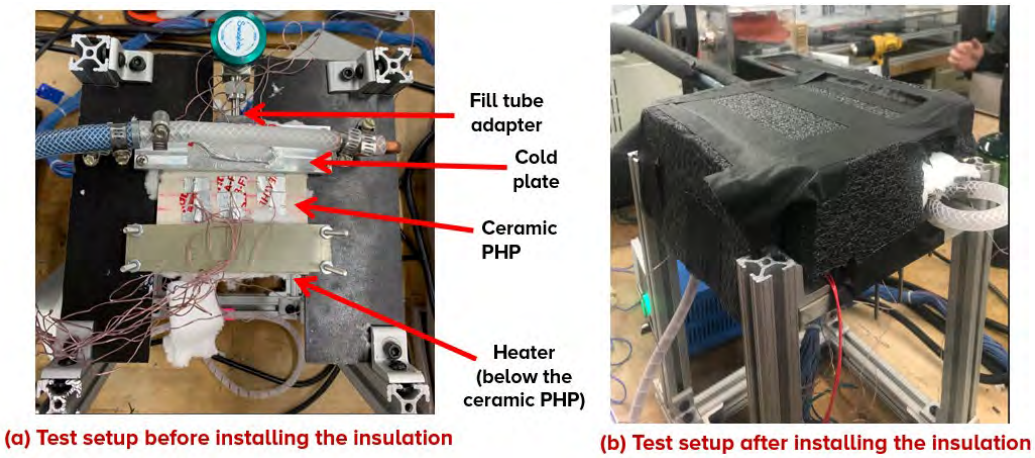

FIGURE 10: EXPERIMENTAL SETUP BEFORE AND AFTER INSTALLING THE INSULATION

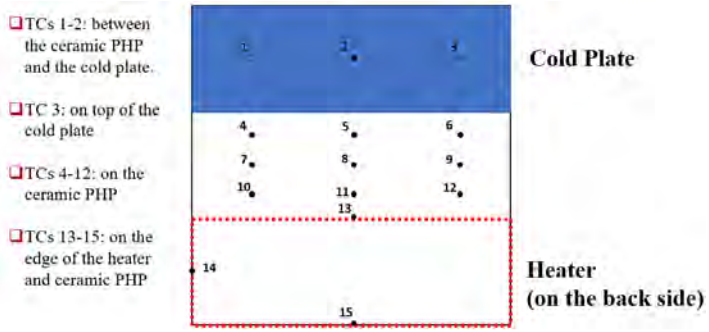

FIGURE 11: LAYOUT OF THE THERMOCOUPLES ON THE CERAMIC PHP

3.1.3. Thermal Testing Results of the 3D Printed Ceramic PHP

- **Testing in the Horizontal Position**

FIGURES 12-13 shows the transient temperature results (thermocouples readings over time) of the baseline case (i.e., empty ceramic PHP) and the charged ceramic PHP, respectively. The temperature difference of the empty and charged ceramic PHP under a power of 30 W, is 118˚C and 49˚C, respectively. A thermal resistance reduction of 58.5% was achieved when using ceramic PHP in the horizontal position under a power of 30 W. The temperature difference is the difference between the heater/evaporator temperature and the cold plate/condenser temperature. TC 15 is selected as the evaporator temperature since its temperature is higher than the other evaporator TCs (i.e., TC13 and TC14). The condenser temperature was selected to be the average of the readings of the three TCs on the condenser side. It was found that, with a fill ratio of 26%, the ceramic PHP can efficiently transport up to 30 W (i.e., 1.43 times the original power). Please note that the PHP experiences a startup behavior before reaching a steady state.

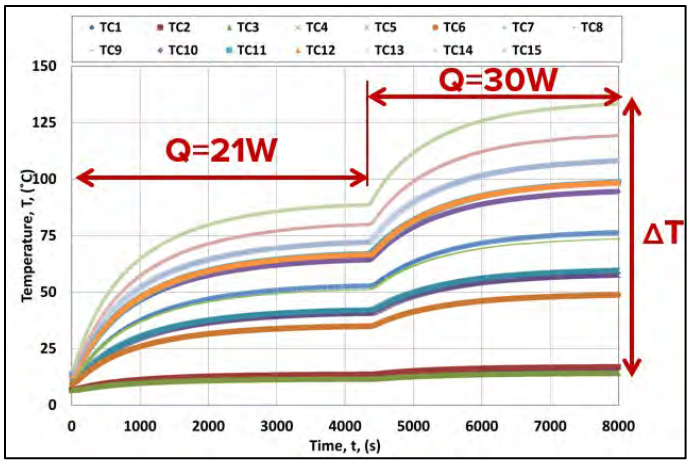

FIGURE 12: TRANSIENT TEMPERATURE RESULTS OF THE EMPTY CERAMIC PHP UNDER HIGHER HEAT INPUT. ΔT IS THE TEMPERATURE DIFFERENCE BETWEEN THE HEAT SOURCE AND HEAT SINK (AT 30 W, ΔT =118˚C).

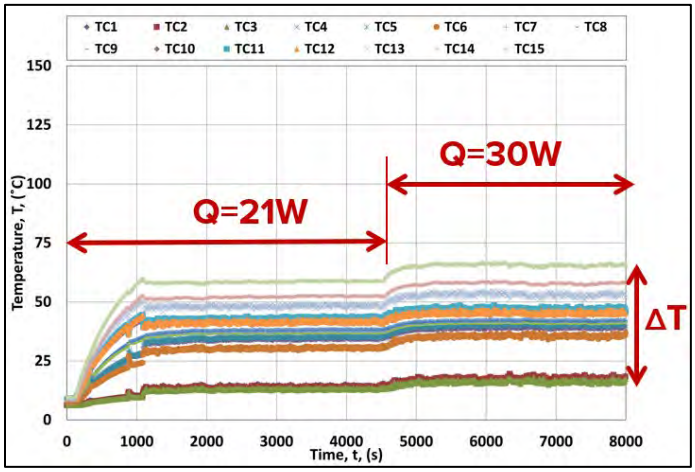

Figure 13: TRANSIENT TEMPERATURE RESULTS OF THE CHARGED CERAMIC PHP UNDER HIGHER HEAT INPUT. THE

CERAMIC PHP IS PARTIALLY FILLED (I.E., 26%). ΔT IS THE TEMPERATURE DIFFERENCE BETWEEN THE HEAT SOURCE AND HEAT SINK (AT 30 W, ΔT =49˚C).

- **Testing under Different Orientations**

In this test, the ceramic PHP was tested under different orientations (i.e., 15˚, 30˚, 90˚). Please note that all the orientations were in the gravity-aided scenario which means the evaporator was always lower than the condenser. The ceramic PHP continued to provide good thermal performance at all orientations. The thermal resistance reductions were 55.66%, 66.5%, and 67.22% at 15˚, 30˚, and 90˚, respectively, when compared to the baseline case. It can be observed that the ceramic PHP provided better thermal performance at larger tilt angles due to the gravity-aided effect. However, at tilt angles larger than 30˚, the thermal performance enhancement is slight. FIGURE 14 concludes the thermal resistance values of the ceramic PHP under different orientations. Please note that the thermal resistance of a solid ceramic plate is added to FIGURE 14 for a more accurate comparison to exclude the effect of the empty channels in the baseline case. It can be observed that the ceramic PHP provided a thermal resistance reduction of 33.2% and 63.2% at the horizontal and vertical positions, respectively, when compared to the solid ceramic plate.

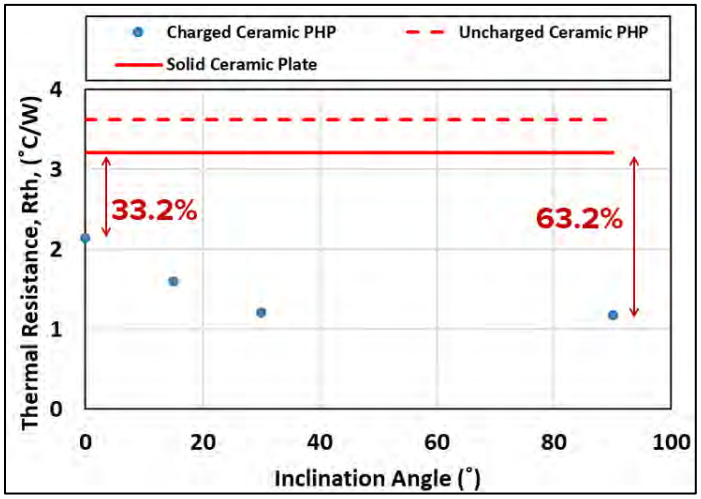

FIGURE 14: THERMAL RESISTANCE VALUES AT DIFFERENT ORIENTATIONS. THE CERAMIC PHP IS PARTIALLY FILLED (i.e., 26%).

3.2. Thermal Testing Results of the Machined Ceramic PHP

The machined ceramic PHP (6" x 6" x 0.32") is bigger than the 3D printed ceramic PHP (4" x 4" x 0.3"). Ceramic machining is a more mature technology (e.g., the capability of fabricating large parts with accurate dimensions) when compared to ceramic 3D printing. In addition, to the best of our knowledge, the ceramic 3D printed PHP developed in this program is the first of its kind. Therefore, smaller prototypes were preferred. The heater (or evaporator) and cold plate (or condenser) areas are 6" x 2" each. FIGURE 15 shows the baseline case. Please note that, for the baseline case, the heat could not be increased more than 70 W due to the temperature limits of the heater and garolite plate. Two thermal tests were performed. For the first test, a fill ratio of 25% was used while the heat input was gradually increased to reach the maximum heat that the ceramic PHP can efficiently transport (FIGURE 16). A similar test was performed for a fill ratio of 42% (FIGURE 17). The ceramic PHP provided significant thermal performance enhancement. For a fill ratio of 25%, a thermal resistance reduction of about 65% and 75% was achieved for heat inputs of 50 W and 70 W, respectively (see FIGURE 15). For a fill ratio of 42%, a thermal resistance reduction of about 54% and 75% was achieved for heat inputs of 50 W and 100 W, respectively (see FIGURE 16). FIGURE 18 concludes the thermal resistance results for the different fill ratios. It can be observed that ceramic PHP tends to provide better performance (e.g., lower thermal resistance) at low fill ratios, however, it can efficiently transport more heat at higher fill ratios.

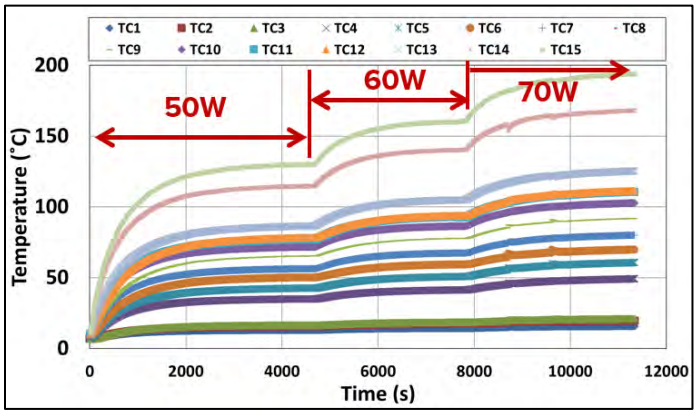

FIGURE 15: TRANSIENT TEMPERATURE RESULTS OF THE EMPTY CERAMIC PHP UNDER DIFFERENT HEAT INPUTS.

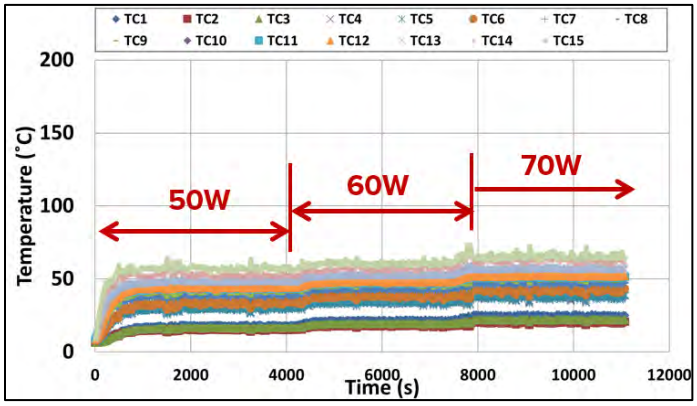

FIGURE 16: TRANSIENT TEMPERATURE RESULTS OF THE CHARGED CERAMIC PHP UNDER DIFFERENT HEAT INPUTS (FIXED FILL RATIO = 25%).

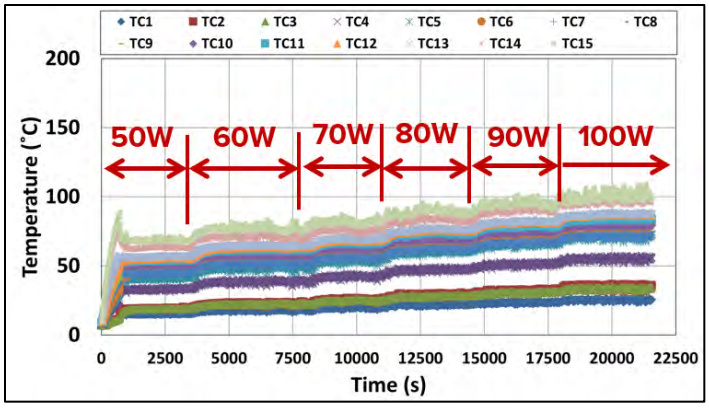

FIGURE 17: TRANSIENT TEMPERATURE RESULTS OF THE CHARGED CERAMIC PHP UNDER DIFFERENT HEAT INPUTS (FIXED FILL RATIO = 42%).

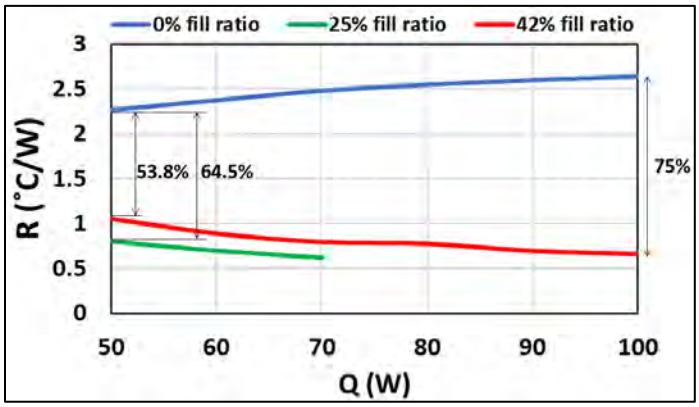

FIGURE 18: THERMAL RESISTANCE VALUES AT DIFFERENT FILL RATIOS AND HEAT INPUTS.

3.3. Electrical Isolation Capabilities of the Ceramic PHP Prototypes

ACT have developed and delivered to UC-Boulder two samples of PHP prototype plates, a 3D printed PHP prototype and a machined PHP prototype. The UC-Boulder team has performed electrical isolation evaluation by electrostatic field simulations and by Hi-Pot tests. FIGURE 19 shows a two-dimensional (2D) setup and field diagram of the simulated PHP prototype. The prototype ceramic is alumina (Al_2O_3) with greater than 78 kV/mm dielectric strength.

Copper plates have been placed on the two sides of the PHP prototype, and voltage has been applied across the plates to evaluate the field distribution in the prototype. With 30 kV applied (relevant medium, the maximum electric field intensity in the alumina and the PHP channels are found to be well below the dielectric strength of the materials. The predicted breakdown voltages for the prototypes were found to be greater than 300 kV for both the case when the PHP channels contain air, and the case when the PHP channels contain fluid (distilled water). FIGURE 20 shows a Hi-Pot electrical test setup. TABLE 2 shows the measured results for the two PHP prototypes. The results show that the prototype sustains up to 30 kV of excitation without corona, discharge, or breakdown events.

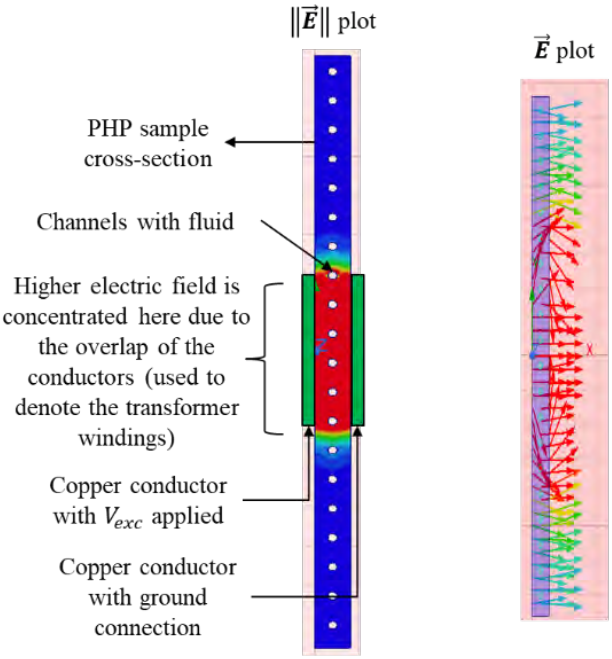

FIGURE 19: TWO-DIMENSIONAL (2D) SETUP AND FIELD DIAGRAM IN THE SIMULATED PHP PROTOTYPE. PROTOTYPE THICKNESS: 8 mm, PHP CHANNEL DIAMETER: 2 mm.

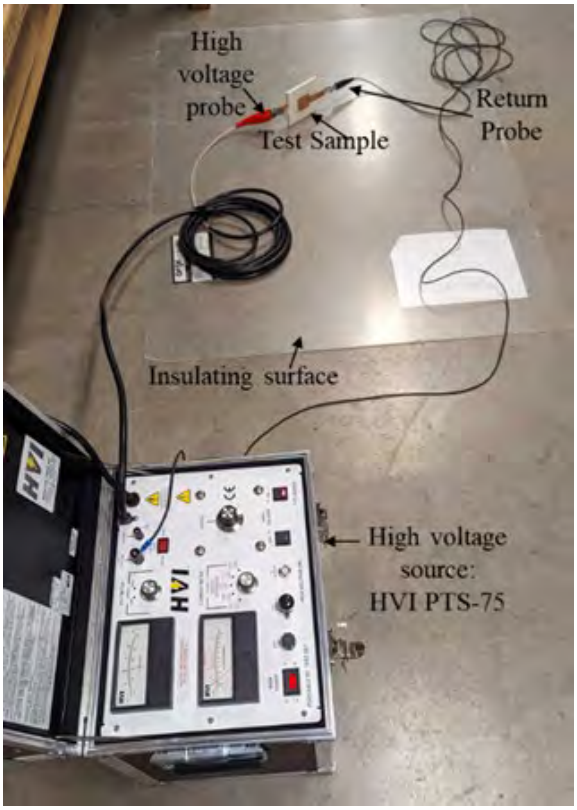

FIGURE 20: ELECTRICAL TESTING OF A PHP PROTOTYPE

TABLE 2: THE ELECTRICAL TESTING RESULTS OF BOTH CERAMIC PHPS

Trial	Applied Voltage (kV)	3D Printed		Machined	
		Current (μA)	Resistance (GΩ)	Current (μA)	Resistance (GΩ)
1	7.5	0.04	187.5	0.045	166.7
2	12.5	0.06	208.3	0.06	208.3
3	15	0.08	187.5	0.075	200
4	20	0.1	200	0.08	250
5	22.5	0.1015	221.7	0.1	225
6	25	0.102	245.1	0.1015	246.3
7	27.5	0.2	137.5	0.2025	135.8

4. CONCLUSIONS

A ceramic PHP was developed to remove the waste heat efficiently and passively from a MV device while maintaining voltage isolation which enables increasing the power density. Two different fabrication methods were investigated. Thermal and electrical testing were performed. The conclusions are summarized below.

- Ceramic PHP prototypes were successfully manufactured via 3D printing and conventional machining methods.
- Successful thermal testing of both 3D printed ceramic PHP and machined ceramic PHP.
  - 3D printed ceramic PHP: thermal resistance reduction= 33%-63%
  - Machined ceramic PHP: thermal resistance reduction= 53%-75%
- Successful electrical testing of both 3D printed ceramic PHP and machined ceramic PHP.
  - Both ceramic PHPs can sustain ≈30 kV of excitation without any breakdown.

ACKNOWLEDGEMENT

This project was funded by the Department of Energy (DOE) under a Phase I Small Business Innovative Research (SBIR) program (Contract: DE-SC0022932). We would like to thank the program manager, Mr. Fernando Salcedo for support and valuable discussions during the program. In addition, special appreciation goes to Eugene Sweigart (Engineering Technician at ACT) who has provided significant contributions during the test setup development.

REFERENCES

[1] "Enabling Fast Charging: A Technology Gap Assessment," U.S. DOE Office of Energy Efficiency, 2017

[2] H. Akachi, "Structure of a Heat Pipe," United States Patent 4921041, 1990.

[3] V. Ayel, M. Slobodeniuk, R. Bertossi, C. Romestant, and Y. Bertin, "Flat plate pulsating heat pipes: A review on the thermohydraulic principles, thermal performances and open issues" Applied Thermal Engineering, 2021

[4] B. Drolen and C. Smoot, "Performance Limits of Oscillating Heat Pipes: Theory and Validation," Journal of Thermophysics and Heat Transfer, vol. 31, no. 4, pp. 920-936, 2017.

[5] B. Taft, A. Williams and B. Drolen, "Working Fluid Selection for Pulsating Heat Pipes," in 42nd AIAA Thermophysics Conference, Honolulu, Hawaii, 2011.

[6] K.L. Lee, S.K. Hota, A. Lutz, and S. Rokkam, "Advanced Two-Phase Cooling System for Modular Power Electronics," 51st International Conference on Environmental Systems (ICES-2022-131) 11-14 July 2022 St. Paul, Minnesota.

[7] S.K. Hota, K.L. Lee, G. Hoeschele, T. Mcfarland, S. Rokkam, R. Bonner, "Experimental Comparison of Two-Phase Heat Spreaders for Space Modular Electronics," 52nd International Conference on Environmental Systems (ICES-2023-332) 16-20 September 2023, Calgary, Canada. (Accepted for presentation and publication).

[8] S.K. Hota, K.L. Lee, G. Hoeschele, and S. Rokkam, "Advanced Cooling System for Modular Electronics Thermal Management," 17th International Heat Transfer Conference (IHT 2023), Cape Town, South Africa. (Accepted for presentation and publication).

[9] S.K. Hota, K.L. Lee, G. Hoeschele, R. Bonner, and S. Rokkam, "Experimental Comparison on Thermal Performance of Pulsating Heat Pipe and Embedded Heat Pipe Heat Spreaders," 40th Annual Semiconductor Thermal Measurement, Modeling and Management Symposium March 25–29, 2024, San Jose, CA.

[10] S.K. Hota, K.L. Lee, B. Leitherer, G. Elias, G. Hoeschele, and S. Rokkam, "Pulsating heat pipe and embedded heat pipe heat spreaders for modular electronics cooling," Case Studies in Thermal Engineering, vol. 49, 2023.

[11] H. Ma, *Oscillating Heat Pipes*, Springer-Verlag, 2015.

[12] R. Nemati and M. Shafii, "Advanced heat transfer analysis of a U-shaped pulsating heat pipe considering evaporative liquid film trailing from its liquid slug," Applied Thermal Engineering, vol. 138, pp. 475-489, 2018.